Supplementary Information for

Impact of Medium-Pore Zeolite Topology on Para-Xylene Production from Toluene Alkylation with Methanol

*Deependra Parmar[1], Seung Hyeok Cha[1,2], Chenfeng Huang[1], Hsu Chiang[4], Seth Washburn[4], Lars C. Grabow[1,3], and Jeffrey D. Rimer[1,]**

[1] William A. Brookshire Department of Chemical and Biomolecular Engineering, University of Houston, 4226 Martin Luther King Boulevard, Houston, Texas 77204, USA
[2] Green Carbon Research Center, Korea Research Institute of Chemical Technology (KRICT), 141 Gajeongro, Yuseong, Daejeon 34114, Republic of Korea
[3] Texas Center for Superconductivity at the University of Houston, 3369 Cullen Blvd., Houston, TX 77204, USA
[4] ExxonMobil Technology and Engineering, 5200 Bayway Drive, Baytown, Texas 77520, USA

*Correspondence sent to: jrimer@central.uh.edu

Table of Contents **Page**

List of Tables and Figures

Supporting Tables

Table S1. Structural properties of zeolite catalysts synthesized in this study.

Catalysts	n-D[a]	Channels (Å)[b]	Maximum Sphere Diam. (Å)[c]		Connectivity
			That can be included	That can diffuse	
ZSM-23	1	4.5 × 5.2	6.19	5.07	Connected
MCM-22	2	4.0 × 5.5, 4.1 × 5.1	9.69	4.92	Independent
TNU-10	2	4.7 × 5.0	6.29	4.94	Connected
ZSM-11	3	5.4 × 5.3	7.72	5.19	Connected
ZSM-5	3	5.1 × 5.5, 5.3 × 5.6	6.36	4.7	Connected
TNU-9	3	5.5 × 5.6, 5.4 × 5.5	8.46	5.39	Connected
IM-5	3	5.5 × 5.6, 5.3 × 5.4, 5.3 × 5.9, 4.8 × 5.4, 5.1 × 5.3	7.34	5.44	Connected

[a]n-D = n-dimensional channels; Diam. = diameter. [b] channel dimensions. [c] Maximum sphere diameter that can fit in pores. All data was obtained from the International Zeolite Association structure database.[1]

Table S2. Acidity determined by pyridine IR for all catalysts studied.

Catalyst	Acidity (pyridine μmol/g)		
	Total	Brønsted	Lewis
ZSM-23	129	112	17
TNU-10	295	239	56
MCM-22	310	186	124
ZSM-11	384	342	42
ZSM-5	319	253	67
TNU-9	526	421	105
IM-5	321	241	80

Supporting Figures

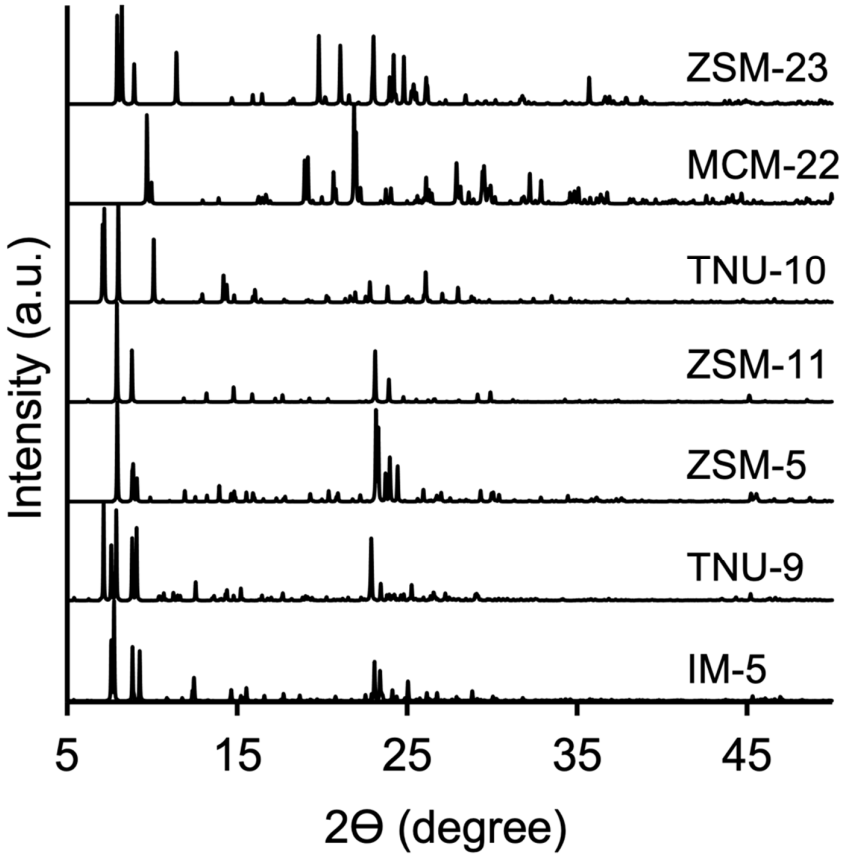

Figure S1. Reference X-ray diffraction (XRD) patterns (obtained from IZA database)[1] for zeolites synthesized in this study. ZSM-5 was the only zeolite purchased from a commercial vendor. These XRD patterns are included for comparative purposes with the experimental XRD patterns of as-synthesized zeolites reported in Figure 1A.

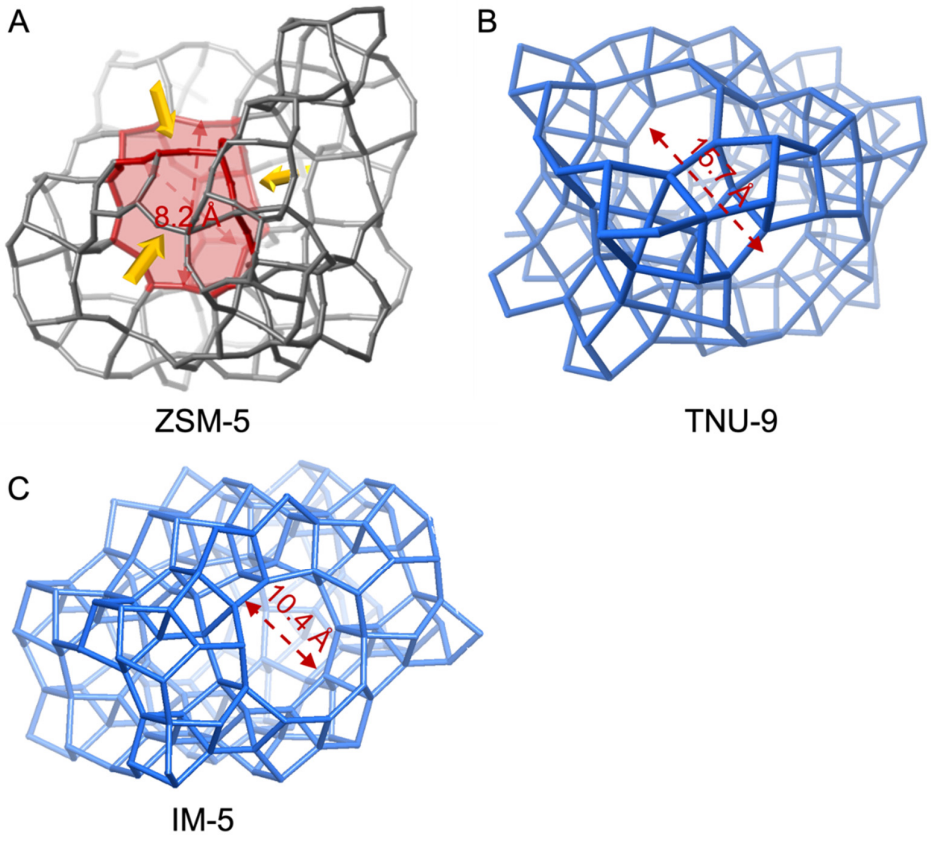

Figure S2. Zeolite frameworks and channel intersections for (A) ZSM-5, (B) TNU-9, and (C) IM-5. Average pore dimensions are labeled in each scheme.

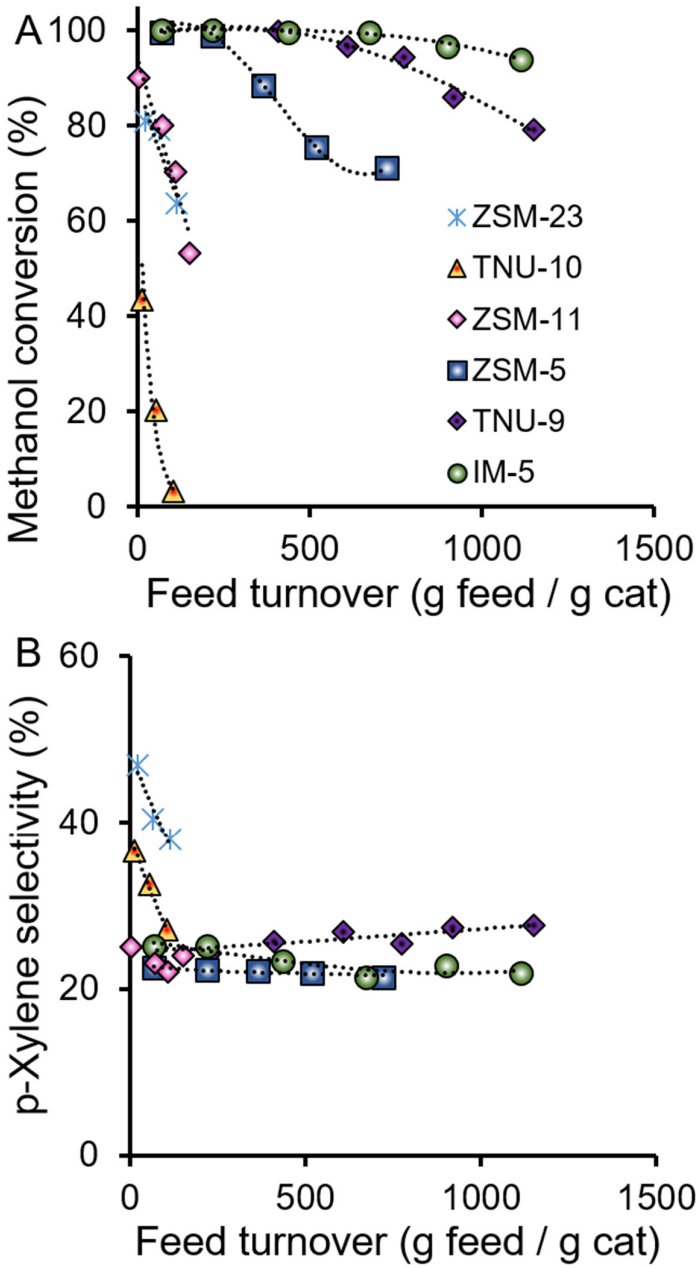

Figure S3. Early time on stream data for trends in Figure 4 of the manuscript, plotted without MCM-22 for improved clarity. (A) Methanol conversion and (B) p-xylene selectivity as a function of feed turnover over medium pore zeolites for toluene alkylation of methanol at 350 °C, 41 atm, toluene-to-methanol ratio of 3, and 30 h^{-1} WHSV.

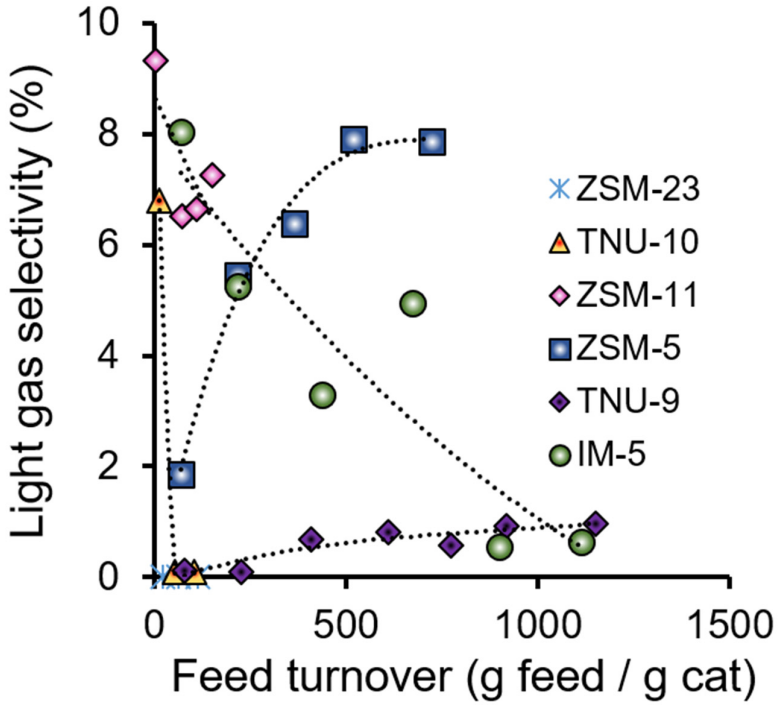

Figure S4. Light gas selectivity for medium pore zeolites as a function of feed turnover for toluene alkylation of methanol at 350 °C, 41 atm, toluene-to-methanol ratio of 3, and 30 h^{-1} WHSV. The values for MCM-22 equal zero for all feed turnover and are omitted for clarity.

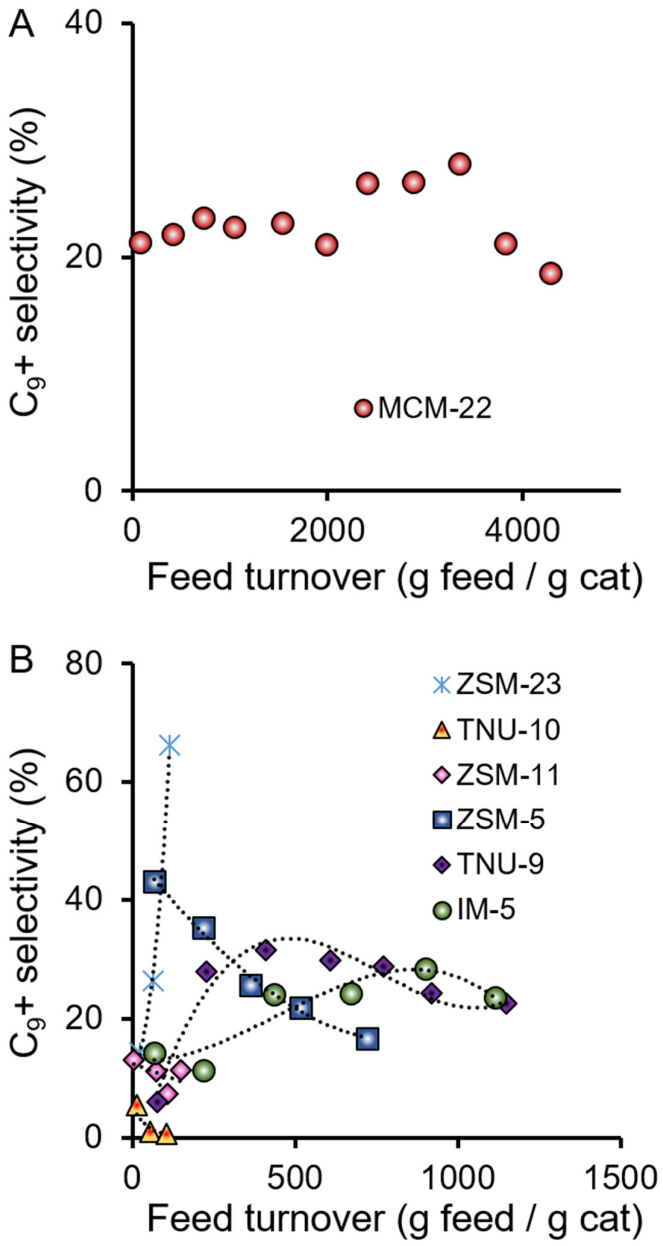

Figure S5. Heavy hydrocarbon (C_{9+}) selectivity for (A) MCM-22 and (B) other medium pore zeolites as a function of feed turnover for toluene alkylation of methanol at 350 °C, 41 atm, toluene-to-methanol ratio of 3, and 30 h^{-1} WHSV. Dashed lines are interpolations to guide the eye.

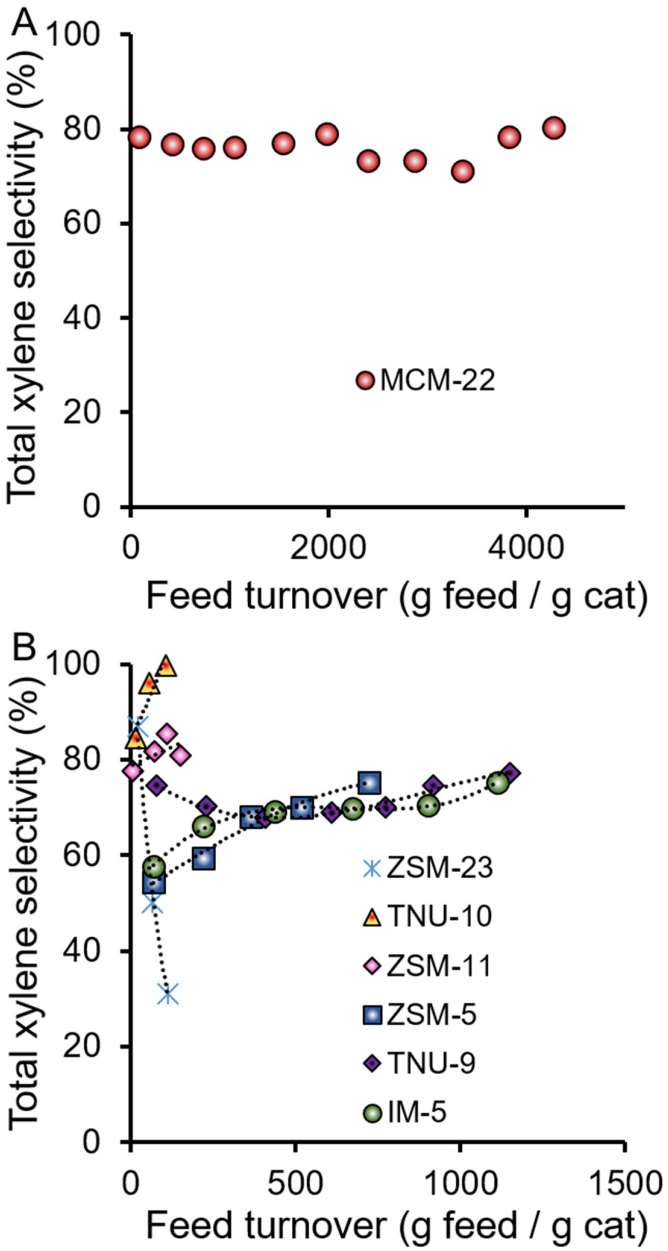

Figure S6. Total xylene selectivity for (A) MCM-22 and (B) other medium pore zeolites as a function of feed turnover for toluene alkylation of methanol at 350 °C, 41 atm, toluene-to-methanol ratio of 3, and 30 h^{-1} WHSV.

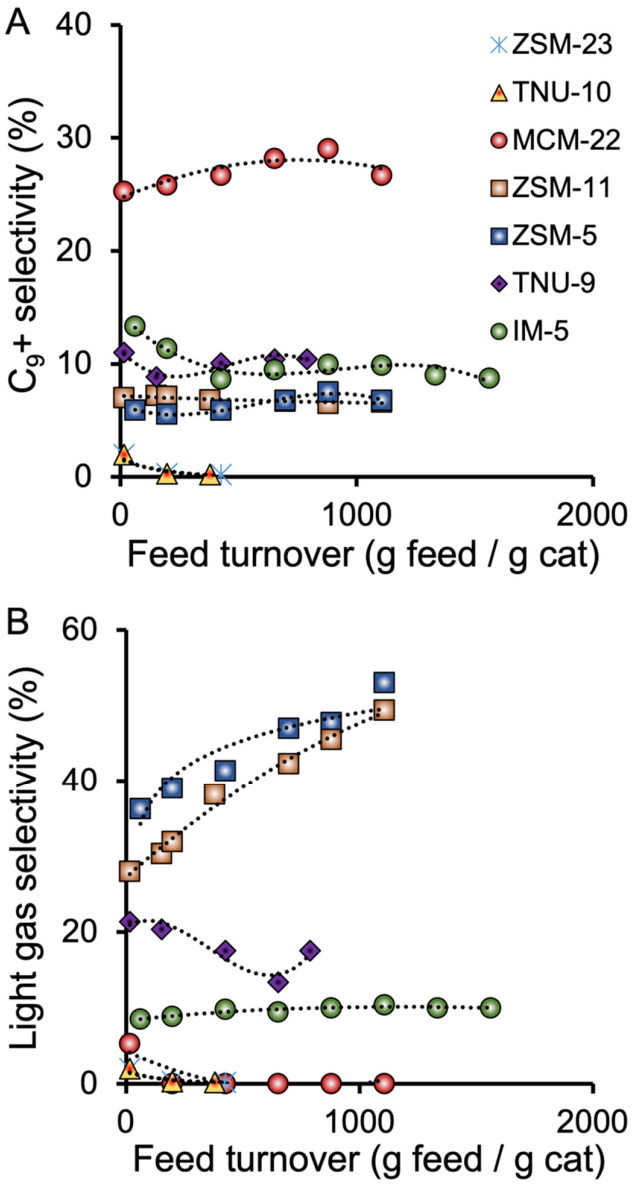

Figure S7. (A) Heavy hydrocarbon (C_9+) and (B) Light gas selectivity as a function of feed turnover over medium pore zeolites for toluene alkylation of methanol at 350 °C, 1 atm, toluene-to-methanol ratio of 3, and 30 h^{-1} WHSV.

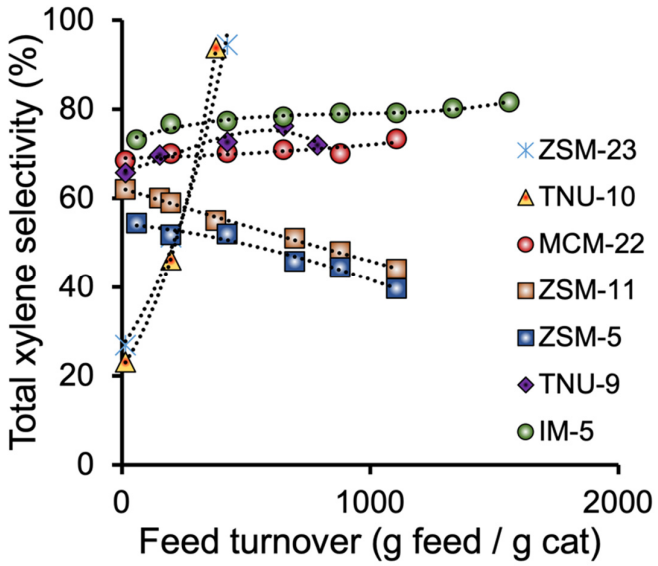

Figure S8. Total xylene selectivity as a function of feed turnover over medium pore zeolites for toluene alkylation of methanol at 350 °C, 1 atm, toluene-to-methanol ratio of 3, and 30 h^{-1} WHSV.

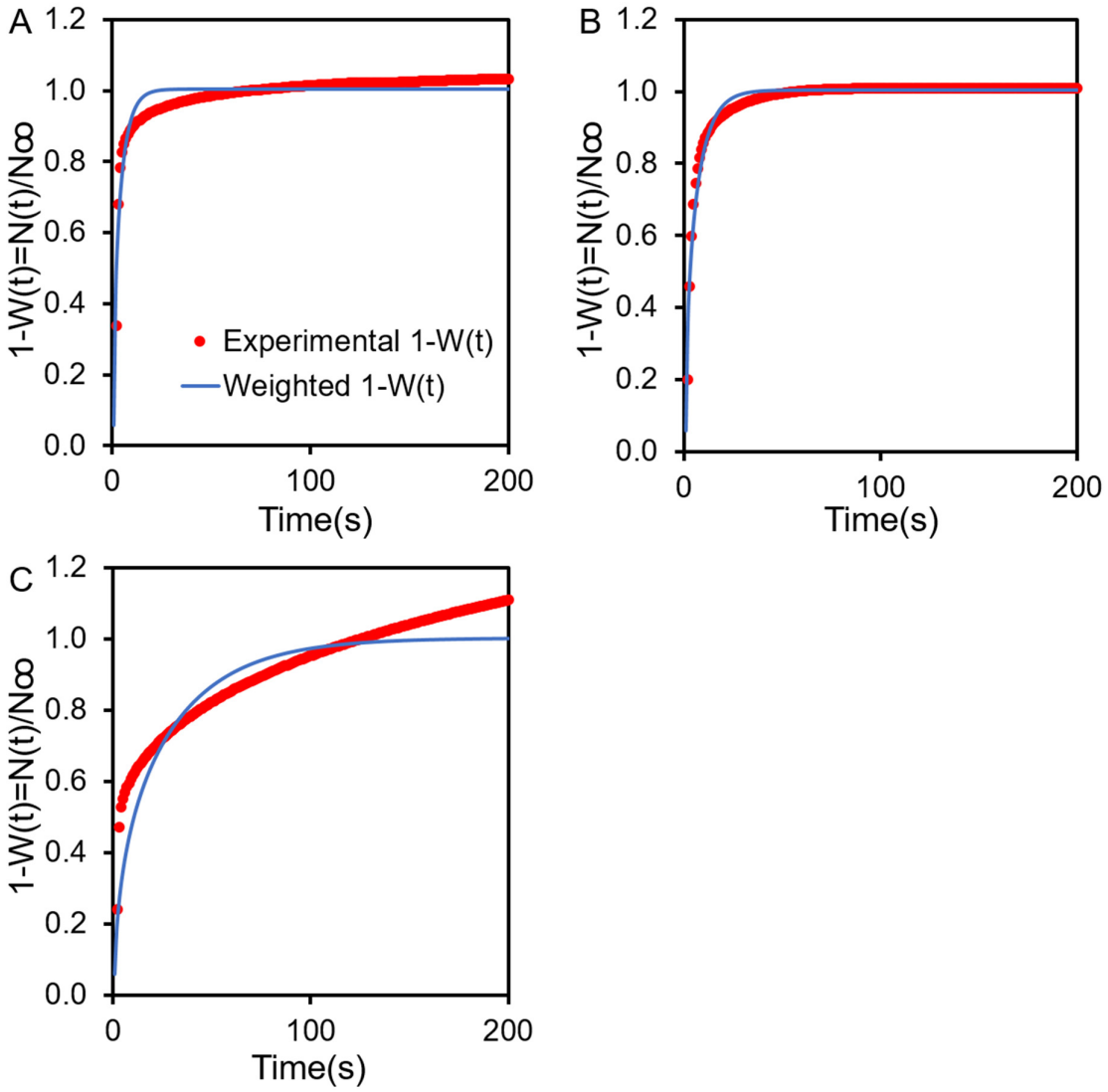

Figure S9. Time-resolved up-take profiles of toluene over pelletized zeolites samples of (A) ZSM-23, (B) TNU-10, and (C) MCM-22, to calculate the mass transport parameter D/R^2 where D is the effective diffusivity and R is a characteristic dimension of the particles in each sample.

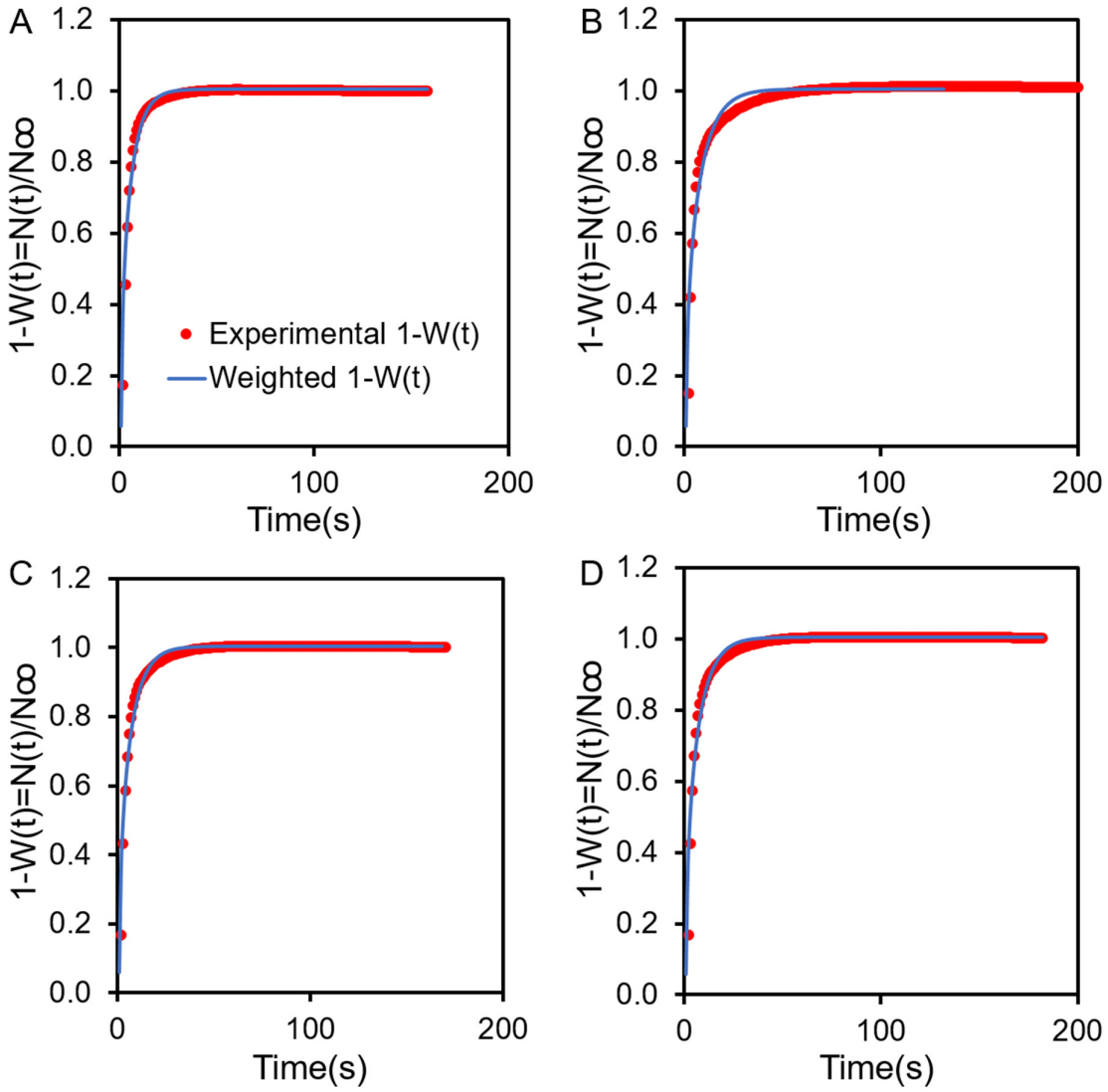

Figure S10. Time-resolved up-take profiles of toluene over pelletized zeolites samples of (A) ZSM-11, (B) ZSM-5, (C) TNU-9, and (D) IM-5, to calculate the mass transport parameter D/R^2 where D is the effective diffusivity and R is a characteristic dimension of the particles in each sample.

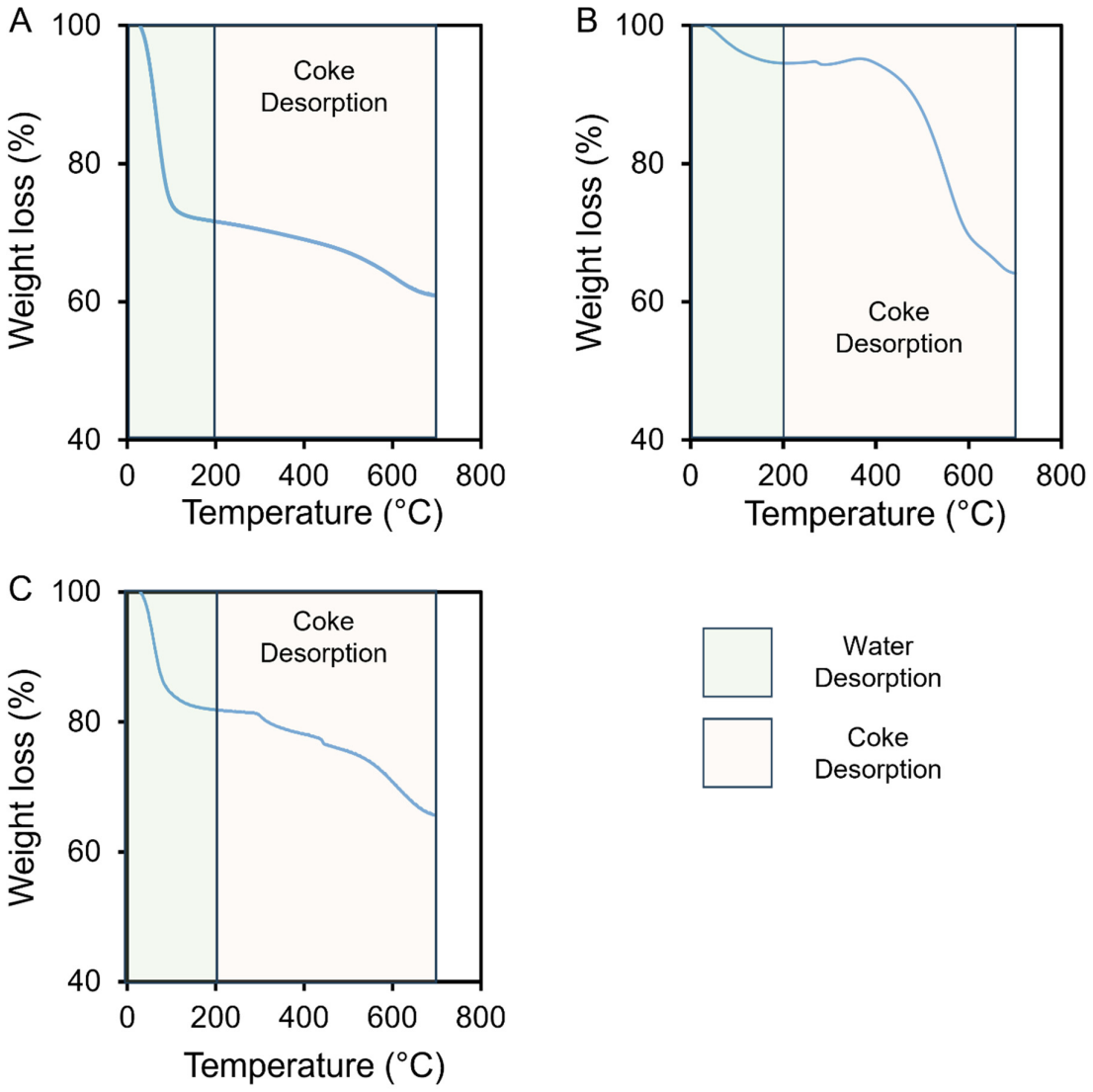

Figure S11. Thermo-gravimetric analysis (TGA) profiles of spent catalysts of (A) ZSM-23, (B) TNU-10, and (C) MCM-22 after the toluene alkylation of methanol at 350 °C, 41 atm, toluene-to-methanol ratio of 3, and 30 h^{-1} WHSV. Weight loss in the region 0 to 200 ºC is attributed to water, while weight loss in the region 200 to 700 ºC is due to coke removal.

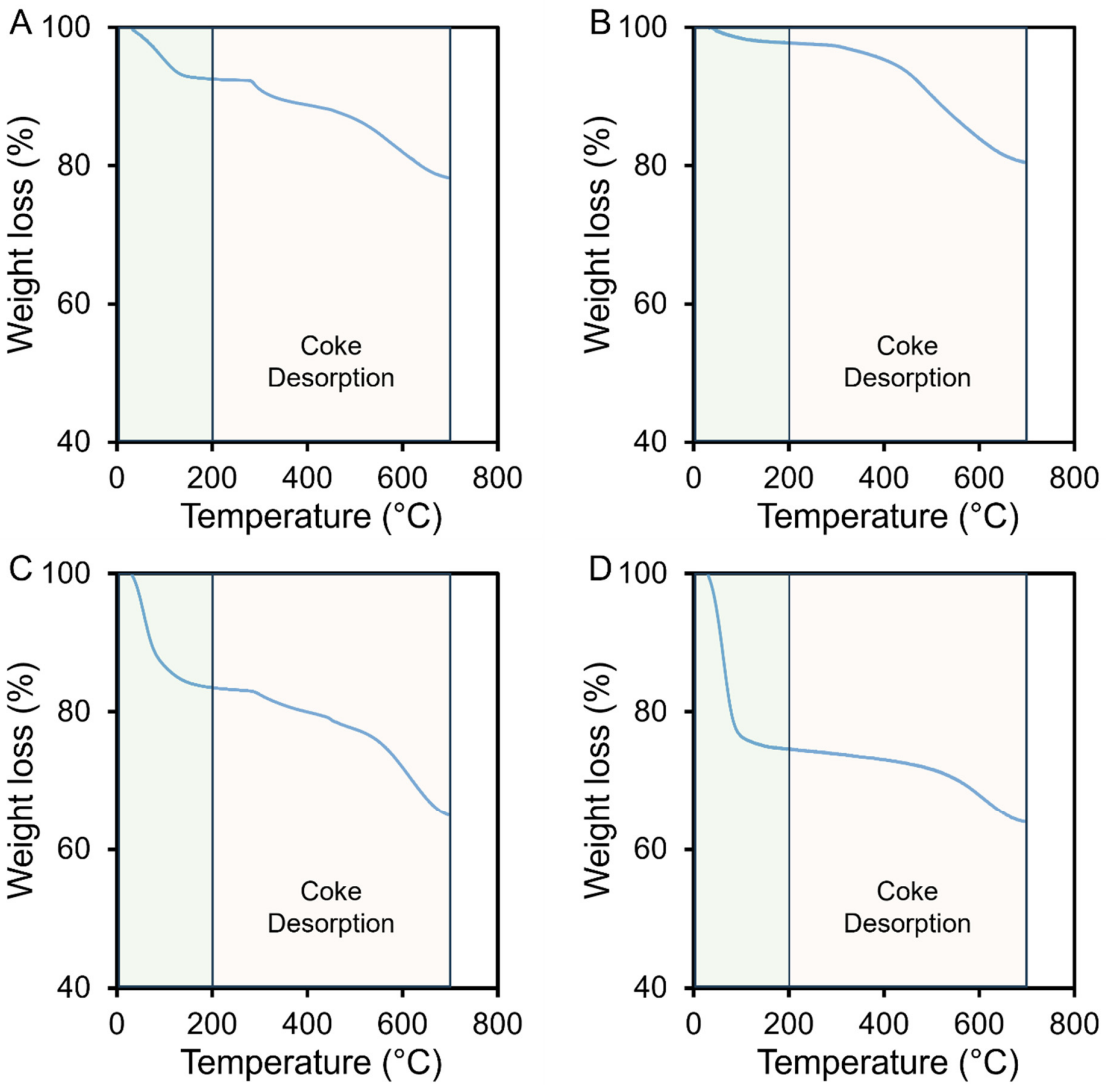

Figure S12. Thermo-gravimetric analysis (TGA) profiles of spent catalysts of (A) ZSM-11, (B) ZSM-5, (C) TNU-9, and (D) IM-5 after the toluene alkylation of methanol at 350 °C, 41 atm, toluene-to-methanol ratio of 3, and 30 h^{-1} WHSV. Weight loss in the region 0 to 200 ºC is attributed to water, while weight loss in the region 200 to 700 ºC is due to coke removal.

References

1 Ch, B. & McCusker, L. Database of Zeolite Structures. *http://www. iza-structure. org/databases* (2015).